



Appendix A

Induction of angiogenesis in a mouse model using engineered transcription factors

EDWARD J. REBAR^{1*}, YAN HUANG^{2*}, REED HICKEY², ANJALI K. NATH², DAVID MEOLI², SAMEER NATH², BINGLIANG CHEN¹, LEI XU¹, YUXIN LIANG¹, ANDREW C. JAMIESON¹, LEI ZHANG¹, S. KAYE SPRATT¹, CASEY C. CASE¹, ALAN WOLFFE¹ & FRANK J. GIORDANO²

¹Sangamo Biosciences, Richmond, California, USA

²Dept. of Medicine, Yale University School of Medicine, New Haven, Connecticut, USA

*These authors contributed equally to this work.

Correspondence should be addressed to F.J.G.; email: ffg9@email.med.yale.edu

Published online 4 November 2002; doi:10.1038/nm795

The relationship between the structure of zinc-finger protein (ZFP) transcription factors and DNA sequence binding specificity has been extensively studied¹. Advances in this field have made it possible to design ZFPs *de novo* that will bind to specific targeted DNA sequences^{2–10}. It has been proposed that such designed ZFPs may eventually be useful in gene therapy^{6,7,10}. A principal advantage of this approach is that activation of an endogenous gene ensures expression of the natural array of splice variants². Preliminary studies in tissue culture have validated the feasibility of this approach^{2–4}. The studies reported here were intended to test whether engineered transcription factors are effective in a whole-organism model. ZFPs were designed to regulate the endogenous gene encoding vascular endothelial growth factor-A (*Vegfa*). Expression of these new ZFPs *in vivo* led to induced expression of the protein VEGF-A, stimulation of angiogenesis and acceleration of experimental wound healing. In addition, the neovasculature resulting from ZFP-induced expression of *Vegfa* was not hyperpermeable as was that produced by expression of murine *Vegfa164* cDNA. These data establish, for the first time, that specifically designed transcription factors can regulate an endogenous gene *in vivo* and evoke a potentially therapeutic biophysiological effect.

A central component of our strategy for designing ZFP transcriptional regulators was the preferential targeting of DNase I-accessible regions within the locus of interest. Such regions are more accessible to transcription factor-sized macromolecules than surrounding DNA, and often comprise binding sites for natural transcriptional regulators. We have found that designing ZFPs to preferentially target such regions yields both a higher success rate and a greater potency of response². Accordingly, we mapped DNase I-accessible regions in the mouse *Vegfa* locus and observed three regions of enhanced accessibility centered approximately at bases –550, +1 and +400 (relative to the transcription start site) (Fig. 1a). We saw similar patterns of accessibility at the *Vegfa* locus in a variety of cell types from human and rat².

Choosing target sites within the ‘+1’ and ‘+400’ accessible regions (Fig. 1b), we designed ZFPs that could recognize these sequences with high affinity (Fig. 1c). To do this we linked together fingers of known triplet preference to yield either three- or six-finger ZFPs with the desired sequence specificities. Two of these designs, designated mVZ+426 and mVZ+509 (according to their target location relative to the transcription start site), con-

tain three fingers and target sequences of nine base pairs conserved in human and mouse. The transcriptional activation properties of these proteins for the corresponding human gene, *VEGFA*, have been described² (referred to as, respectively, VZ+434 and VZ+42+/+530 in that study). ZFP mVZ+57 contains six fingers and targets a sequence of 18 base pairs present only in the mouse. Gel-shift assays confirmed high-affinity binding of these specific ZFPs to their targeted *Vegfa* regulatory sequences (Fig. 1d). We constructed cytomegalovirus promoter (CMV)-driven expression plasmids encoding ZFP-based *Vegfa*-activating transcription factors by fusing sequences encoding the finger domains with the herpes simplex virus VP16 transactivation domain, a nuclear translocation signal and a FLAG epitope (Fig. 1e).

To test the ability of these ZFPs to activate *Vegfa* expression *in vitro*, we stably introduced ZFP expression cassettes into C127I cells by retroviral transduction. ZFP expression in these cells resulted in transcriptional upregulation of the endogenous *Vegfa* locus and secretion of VEGF-A (Fig. 1f,g). It has previously been shown that ZFP activation of *Vegfa* leads to production of the naturally occurring splice variants in their normal stoichiometry². The intensity of *Vegfa* activation varied depending on the promoter region targeted.

The configuration of the chromatin encompassing a particular gene may vary among cell types and in response to the environment of the cell¹¹. Given that transcription factors generally require a ‘permissive’ chromatin configuration for DNA binding and that the chromatin configuration *in vivo* might vary considerably from that existing *in vitro*, it was not known whether these artificial ZFP-based transcription factors could activate *Vegfa* and induce angiogenesis *in vivo* (in this context referring to events occurring within a living animal). To examine this, we inserted the mVZ+509, mVZ+57 and mVZ+426 expression cassettes into recombinant adenovirus vectors. Injection of these adeno-ZFP vectors into the quadriceps muscle of CD-1 mice resulted in substantially greater VEGF-A expression than did contralateral quadriceps injection with adenovirus carrying the gene encoding green fluorescent protein (adeno-GFP) (Fig. 2a–c). To ensure that *Vegfa* activation was not influenced by the presence of the adenovirus, this experiment was repeated with injections of plasmid DNA encoding the various *Vegfa*-activating ZFPs. To ensure that a nonspecific effect of ZFP expression or binding was not contributing to the *Vegfa* activation, a plasmid encoding the

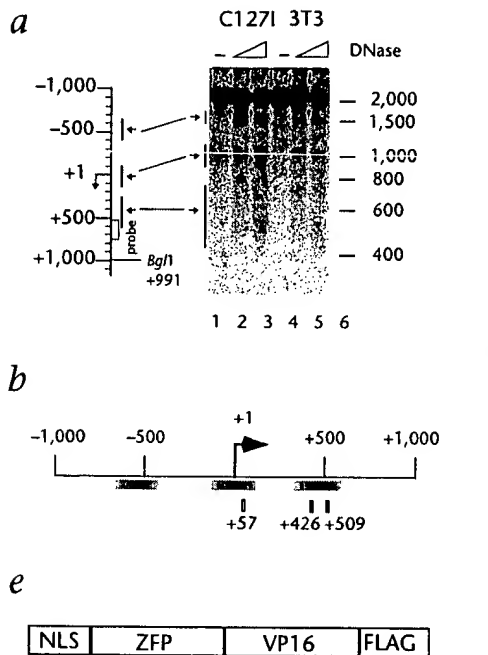
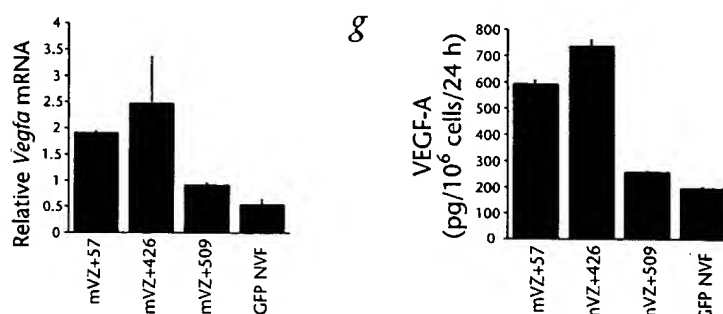


Fig. 1 Targeting, design and *in vitro* analysis of zinc-finger proteins designed for the mouse *Vegfa* locus. **a**, Mapping of DNase I-accessible regions in the mouse *Vegfa* promoter region. Vertical bar, *Vegfa* promoter region; hooked arrow, transcription start site. Tick marks indicate units of 100 bp. The migration pattern for a set of DNA standard fragments is indicated on the right, with the size of each fragment given in base pairs. Arrows highlight the relationship of observed bands to location of accessible chromatin regions relative to the *Vegfa* transcription start site. DNase I concentrations (units/ml) in lanes 1–6 were as follows: 0, 32, 64, 0, 8 and 16. **b**, Location of ZFP target sites. A schematic representation of the mouse *Vegfa* gene is provided, showing the location of the transcription initiation site (arrow) and the DNase I-accessible regions (gradient-filled rectangles) determined in these studies. ZFP target locations are indicated by dashes and the position of the upstream edge of each ZFP target is indicated by the number below it. Numbering is relative to the start site of transcription (+1). **c**, ZFP target sequences and finger designs. ZFPs are named according to target site location and the suffix mVZ (for mouse *Vegfa* ZFP). Finger designs indicate the identity of amino acid residues at positions '−1' to '+6' of the alpha helix of each finger. **d**, Gel-shift assays of target affinity. A 3-fold dilution series of each protein was tested for binding to its DNA target, with the highest concentration in lane 10 and the lowest concentration in lane 2.

Fig. 1 Targeting, design and *in vitro* analysis of zinc-finger proteins designed for the mouse *Vegfa* locus. **a**, Mapping of DNase I-accessible regions in the mouse *Vegfa* promoter region. Vertical bar, *Vegfa* promoter region; hooked arrow, transcription start site. Tick marks indicate units of 100 bp. The migration pattern for a set of DNA standard fragments is indicated on the right, with the size of each fragment given in base pairs. Arrows highlight the relationship of observed bands to location of accessible chromatin regions relative to the *Vegfa* transcription start site. DNase I concentrations (units/ml) in lanes 1–6 were as follows: 0, 32, 64, 0, 8 and 16. **b**, Location of ZFP target sites. A schematic representation of the mouse *Vegfa* gene is provided, showing the location of the transcription initiation site (arrow) and the DNase I-accessible regions (gradient-filled rectangles) determined in these studies. ZFP target locations are indicated by dashes and the position of the upstream edge of each ZFP target is indicated by the number below it. Numbering is relative to the start site of transcription (+1). **c**, ZFP target sequences and finger designs. ZFPs are named according to target site location and the suffix mVZ (for mouse *Vegfa* ZFP). Finger designs indicate the identity of amino acid residues at positions '−1' to '+6' of the alpha helix of each finger. **d**, Gel-shift assay of target affinity. A 3-fold dilution series of each protein was tested for binding to its DNA target, with the highest concentration in lane 10 and the lowest concentration in lane 2.

ZFP Name	Target		Finger designs				
	Sequence 5'-3'	Subsites 5'-3'	-1	2	3	4	5
mVZ+57	TGAGCGGGCGGCAGCGGAGc	TGAG GCCG GCCG GCAg GCGG GAGC	QSGHLTK RSDELTSR RSDELTR QSGSILTR RSDELQR RSDELAK	F6 F5 F4 F3 F2 F1			
mVZ+426	GGGGGTGACc	GGGg GGTg GACC	RSDHLSR TSGHLVR DRSILTR	F3 F2 F1			
mVZ+509	GCTGGGGGCg	GCTg GGGg GGCg	QSSDLTR RSDHLTR DRSILTR	F3 F2 F1			

ZFP	Target	Gel shift	Apparent K_d (nM)
mVZ+57	TGAGCGGGCGGCAGCGGAGc	Bound Free	0.031
mVZ+426	GGGGGTGACc	Bound Free	<0.01
mVZ+509	GCTGGGGGCg	Bound Free	<0.01
SP1	GGGGCGGGGg	Bound Free	0.053



Lane 1 contains probe alone. Apparent K_d values, derived from the average of 3 such studies, are indicated at right. **e**, Schematic representation of the ZFP transcriptional activators used in these studies. 'NLS', 'VP16' and 'FLAG' indicate the relative locations of, respectively, a nuclear localization signal, VP16 transactivation domain and FLAG tag. **f**, ZFP-mediated activation of *Vegfa* transcription *in vitro*. Mouse-derived C127I cells were stably transduced with retroviral vectors encoding each ZFP transcriptional activator or a control protein in which GFP was substituted for the ZFP DNA-binding domain. RT-PCR analysis is expressed as relative *Vegfa* mRNA. GAPDH served as a loading control. **g**, As in (f), except that the amount of secreted VEGF-A protein was quantified by ELISA.

finger region of mVZ+57 without the VP16 transactivation domain was injected into the contralateral quadriceps as a control. These studies showed the expected *in vivo* activation of *Vegfa* by the designed ZFP and substantiated the notion that this activation was not a general response to the presence of the fingers but also required the VP16 transactivation domain (Fig. 2d).

To gain an initial sense of the magnitude and selectivity of *in vivo* *Vegfa* activation by our ZFP activators, we carried out quantitative RT-PCR analysis of RNA isolated from virus-treated quadriceps. In addition to *Vegfa*, these studies quantified relative expression of three non-target genes: *Glut1* (also known as *Slc2a1*),

Pgk1 and *Ldh1*, encoding glucose transporter-1, phosphoglycerate kinase and the A chain of lactate dehydrogenase-1, respectively. These genes are actively transcribed in skeletal muscle and would therefore be expected to present accessible chromatin regions capable of binding transcription factors. These genes are also induced by the hypoxic response, and were chosen to control for the possibility that our ZFPs were activating *Vegfa* by indirect effects acting through this pathway. Adenovirus encoding mVZ+57 was injected into the quadriceps muscle of CD-1 mice as above ($n = 4$ per group). Evaluation of gene expression three days later by real-time quantitative RT-PCR showed 266.7% ($P = 0.005$) more

Vegfa mRNA in mVZ+57-injected muscle as compared to adenovirus-GFP-injected contralateral controls (Fig. 2e). In contrast, mVZ+57 did not activate *Ldh1* or *Glut1* and activated *Pgk1* only slightly. As a positive control, an adenovirus encoding the hypoxia-inducible

transcription factor HIF-1 α was similarly tested and showed markedly greater expression of all these genes (Fig. 2e).

Further studies investigated effects of mVZ+509 and mVZ+426 on vascularization in the mouse ear angiogenesis model¹².

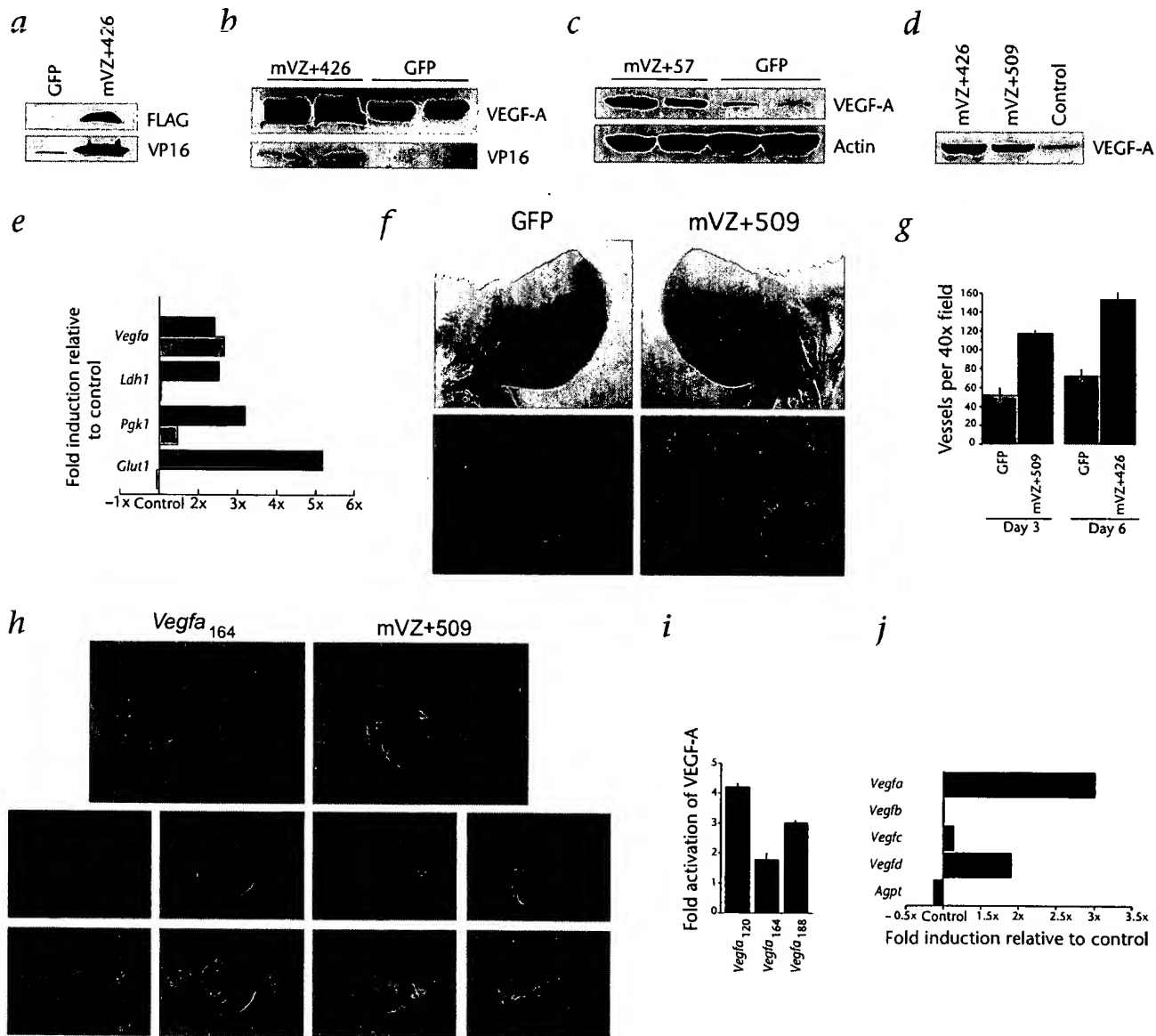


Fig. 2 ZFP-mediated *Vegfa* activation and induction of angiogenesis *in vivo*. **a**, Western blotting of smooth muscle cells transduced with adenovirus encoding *Vegf*-ZFP; the presence of FLAG epitope and VP16 transactivation domain (TAD) demonstrates effective expression of the *Vegf*-ZFP. **b, c**, Western blots showing VEGF-A in the quadriceps muscle of CD-1 mice 3 d after intramuscular injection with 10^8 PFU of adenovirus encoding either mVZ+426 or mVZ+57. VP16 TAD expression documents expression of the ZFP; actin expression documents equal loading. **d**, Western blot of *Vegfa* expression in skeletal muscle 3 d after injection of plasmid DNA encoding either mVZ+426, mVZ+509 or a control plasmid encoding a *Vegfa*-targeting finger region without the VP16 TAD. **e**, Comparison of profiles of gene activation induced by *Vegf*-ZFP mVZ+57 (light bars) and transcription factor HIF-1 α (dark bars). Real-time RT-PCR shows that injection of adenovirus encoding human HIF-1 α into the quadriceps muscle results in significant increases ($P \leq 0.01$) in the amounts of mRNAs for phosphoglycerate kinase (*Pgk1*), the glucose transporter (*Glut1*) and the lactate dehydrogenase A chain (*Ldh1*) as well as activation of *Vegfa*. In contrast, mVZ+57 activates *Vegfa* without activation of *Glut1* or *Ldh1* and with only a minimal increase in *Pgk1* expression ($n = 4$ per group; all values compared to contralateral control quadriceps injected with adenovirus-GFP). **f, g**, *Vegfa*-activating ZFP expression induces angiogenesis in the mouse ear. Subcutaneous injection of adenovirus encoding mVZ+509 results in visible neovascularization after 3 d relative to contralateral ear injected with adenovirus encoding GFP. Quantification by immunohistochemical vessel counts 3 d after mVZ+509 ($n = 5$) and 6 d after mVZ+426 ($n = 4$) corroborates the neovascularization. In **g**, $P < 0.001$ (left); $P = 0.001$ (right). **h**, In similar experiments, angiogenesis stimulated by mVZ+509 (top and middle right) does not produce a hyperpermeable neovasculature as determined by Evans blue dye extravasation (bottom right). The neovasculature induced by *Vegfa*₁₆₄ adenovirus transduction (left) shows spontaneous hemorrhage and Evans blue extravasation. **i**, Quantitative RT-PCR shows increases in mRNA of all 3 major *Vegfa* splice variants *in vivo* 3 d after VEGF-ZFP transduction. **j**, RT-PCR shows increased total *Vegfa* mRNA, no substantial increases in *Agpt* (angiopoietin), *Vegfb* or *Vegfc* mRNAs, and a moderate increase in *Vegfd* mRNA in response to mVZ+509 ZFP transduction.

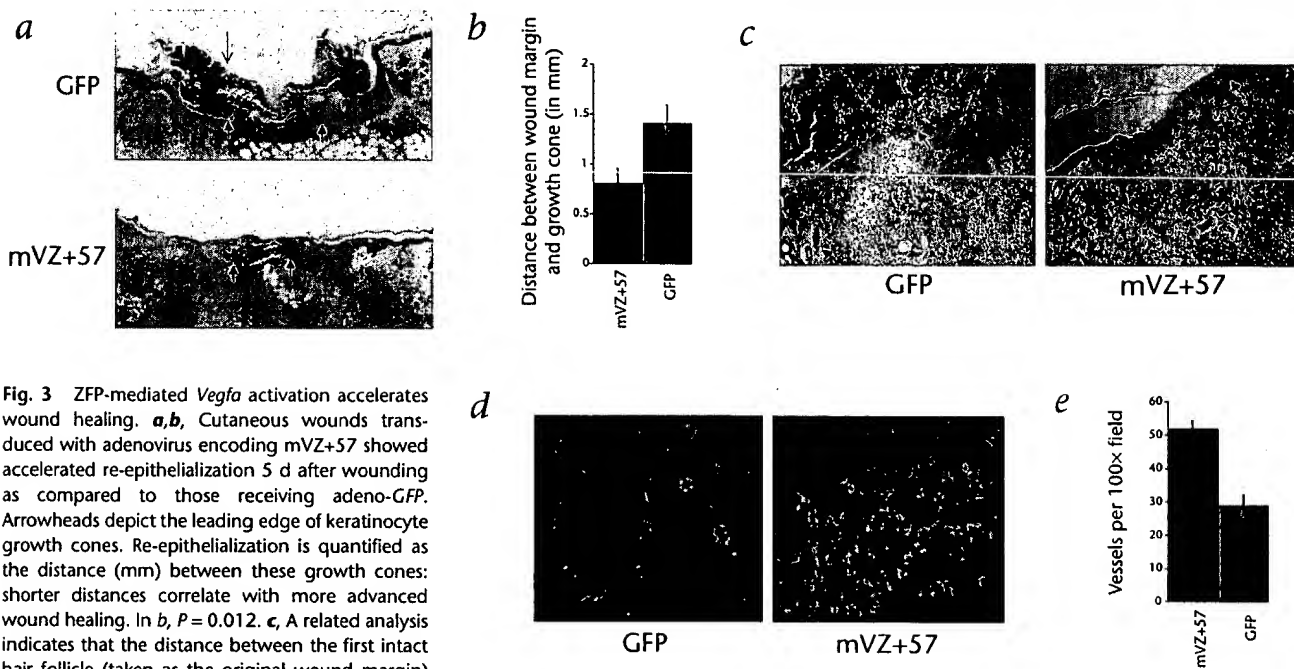


Fig. 3 ZFP-mediated *Vegfa* activation accelerates wound healing. **a, b**, Cutaneous wounds transduced with adenovirus encoding mVZ+57 showed accelerated re-epithelialization 5 d after wounding as compared to those receiving adeno-GFP. Arrowheads depict the leading edge of keratinocyte growth cones. Re-epithelialization is quantified as the distance (mm) between these growth cones: shorter distances correlate with more advanced wound healing. In **b**, $P = 0.012$. **c**, A related analysis indicates that the distance between the first intact hair follicle (taken as the original wound margin) and the keratinocyte growth cone is greater in the mVZ+57-treated wounds (arrows), indicating more rapid re-epithelialization. **d–e**, Endothelial cell immunostaining of the same wounds shows an increase

in vessel counts in the mVZ+57-transduced wounds at day 5 as compared to the GFP-transduced control wounds. In **e**, $P < 0.001$.

Subcutaneous injection of either construct in the external ear of CD-1 mice resulted in definitively greater vascularity in the ZFP-treated ears as compared to contralateral ears injected with adeno-GFP (Fig. 2f). These differences were readily apparent visually and were corroborated by immunohistochemical vessel counting: mVZ+509 111 ± 9.2 versus GFP 43.8 ± 7.7 per 100x field 3 days after transduction ($P = 0.005$, $n = 5$); mVZ+426 153.7 ± 10.0 versus GFP 74.7 ± 6.6 per 100x field 6 days after transduction ($P = 0.001$, $n = 4$) (Fig. 2g). VEGF-A is a potent vascular permeability factor that induces hemorrhage and extravasation of intravascular dye in the mouse ear model¹². Notably, in contrast to the vasculature of ears similarly treated with an adenovirus carrying murine *Vegfa*₁₆₄ cDNA, the ZFP-induced neovasculature was not spontaneously hemorrhagic and was not permeable to infusion of Evans blue dye (Fig. 2h). Real-time quantitative RT-PCR of RNA isolated from treated and control ears showed ZFP-mediated increases in all three principal *Vegfa* splice variants but no increase in the mRNA for angiopoietin, a growth factor previously shown to be capable of promoting the growth of a more 'mature' non-leaky neovasculature (Fig. 2i,j)¹³. Similarly, there was no apparent induction of *Vegfb* or *Vegfc*, although the amount of *Vegfd* (Fig. f) mRNA was 1.91 ± 0.27 -fold greater than in controls.

To further examine the *in vivo* biological effects of these *Vegfa*-regulating ZFPs, we carried out adeno-mVZ+57 gene transfer into cutaneous wounds in a mouse model of wound healing¹⁴. Five days after wounding and gene transfer, wounds treated with adeno-mVZ+57 showed markedly accelerated re-epithelialization as quantified by the measured distance between keratinocyte growth cones: *Vegfa*-ZFP 0.8 ± 0.14 mm versus adeno-GFP 1.42 ± 0.15 mm ($P < 0.012$, $n = 6$ per group) (Fig. 3a–c). This was accompanied by a 63.4% greater vessel density in the ZFP-treated wounds as compared to GFP-treated control wounds in the same mouse ($P < 0.01$, $n = 5$) (Fig. 3d,e).

In these studies we demonstrate, for the first time, the feasibility of regulating genes and complex biological processes *in vivo* using engineered ZFP-based transcription factors. This represents a new paradigm in gene therapy that is predicated on the modulated expression of endogenous genes. There are considerable potential advantages to this approach, including the ability to regulate all the natural splice variants of an endogenous gene with a single deliverable effector molecule². The *Vegfa* gene encodes a number of splice variants, and recent data suggest that these are not functionally equivalent or redundant¹⁵. In this study we show that the neovasculature resulting from activation of the endogenous *Vegfa* by engineered ZFPs is not hyperpermeable, as is that resulting from *Vegfa*₁₆₄ alone. It is possible that the ZFP-induced neovasculature is more physiologically mature and that this is due to the induced expression of the natural *Vegfa* splice variants. This hypothesis is supported by recent findings indicating that transcriptional upregulation of the endogenous *Vegfa* by the hypoxia-inducible factor HIF-1 α also produces a non-hyperpermeable neovasculature¹⁶. It is also possible that another factor, not specifically targeted by the *Vegfa*-activating ZFPs, is upregulated in response to ZFP expression and contributes to the vascular phenotype. Expression of angiopoietin, an angiogenic factor capable of inducing a non-hyperpermeable neovasculature, is not induced in *Vegfa*-ZFP-transduced tissue. Expression of the VEGF family members VEGF-B and VEGF-C is also unresponsive to ZFP transduction, although that of VEGF-D was increased to a modest degree, albeit to a lesser extent than for the targeted VEGF-A. The reasons for the relatively small increase in VEGF-D are unclear. There are partial binding sites for mVZ+509 in the murine *Vegfd* promoter that may allow activation. It is also possible that these increases are secondary to the induced expression of VEGF-A. Despite this increase in VEGF-D expression, the total amount of *Vegfd* mRNA remained less than

approximately 1/12 that of *Vegfa* mRNA (data not shown). Whether this is enough to contribute substantively to the vascular phenotype is unknown.

Another advantage of ZFP-based gene regulation is that it facilitates the simultaneous regulation of multiple separate genes with a single therapeutic intervention. In especially favorable cases, this can be accomplished by designing a single ZFP that binds a DNA sequence common to all the desired genes. It can also be accomplished by combining expression cassettes encoding multiple ZFP constructs into a single gene-delivery vehicle. The relatively small size of these ZFP cassettes (~0.6–1.0 kb) facilitates the latter approach. Regulating multiple genes and their natural splice variants using a cDNA-based approach would be distinctly more difficult. This ability to regulate multiple endogenous genes through a single molecular intervention may prove very advantageous for the therapeutic modulation of complex biological processes that involve the coordinated expression of multiple genes. Currently, approaches to stimulate angiogenesis in ischemic hearts are based on the expression of single isoforms of angiogenic growth factors^{17–19}. The ability to activate expression of multiple angiogenic genes and their splice variants with a single delivery vehicle, such as is facilitated by the ZFP-based approach, might provide a distinct advantage in the therapeutic regulation of angiogenesis. Establishing this, however, will require more extensive analysis in multiple *in vivo* models such as the ameroid model of coronary insufficiency and the hindlimb ischemia model^{17,20}. Revascularization in these settings is complex, and whether ZFP-induced expression of *Vegfa* splice variants will be advantageous in such settings is currently unknown.

One crucial finding of the current study is the demonstration that synthetic transcription factors targeted to open regions of chromatin can specifically regulate targeted endogenous genes *in vivo*. We have previously shown that similar ZFP-based constructs can effect gene activation *in vitro*, but this was in the context of transformed and immortalized cell lines with a chromatin structure which may be different from that encountered in quiescent muscle cells *in vivo*. These data demonstrate, for the first time, the crucial next step: gene activation and induction of a therapeutic biophysiological effect by an engineered ZFP transcription factor *in vivo*.

A crucial issue with respect to the use of designed transcription factors is specificity *in vivo*. As an initial step towards addressing this issue, our muscle studies included analyses of a set of non-target genes. The loci examined in these studies were chosen because they are transcribed in muscle (and therefore should contain accessible chromatin regions) and also because they are targets for the hypoxic response. We found little or no ZFP activation of these genes. In contrast, and as expected, these genes were activated by an adenovirus encoding HIF-1 α , an endogenous transcription factor that is being developed as a potential pro-angiogenic gene-therapy agent²⁰.

ZFP-based transcription factors can be designed to activate, or when combined with a repression domain, to repress expression of nearly any endogenous gene. The inherent generality and versatility of this approach has notable implications for gene-based therapies predicated on the regulation of complex biological processes such as angiogenesis. These studies establish, for the first time, the feasibility and potential utility of this approach *in vivo*.

Methods

Mapping of DNase I-accessible regions of chromatin in the mouse *Vegfa* locus.

Nuclei were isolated from C127I and NIH3T3 cells (ATCC,

Manassas, Virginia) and treated with DNase I (Worthington, Lakewood, New Jersey) as previously described³ except that digests were for 1.5 min at 22 °C (DNase I concentrations as indicated in Fig. 1). Genomic DNA isolation, restriction enzyme digestion and Southern-blot analysis were done as described³ with enzymes and probes as indicated in Figure 1.

Synthesis of ZFP genes and ZFP binding studies. The assembly of genes encoding the three-finger ZFPs mVZ+426 and mVZ+509 has been described² (VZ+434 and VZ+42+/+530, respectively, in that study). The gene encoding the six-finger protein mVZ+57 was assembled by joining genes encoding fingers 1–3 and 4–6 with a short DNA spacer encoding a flexible peptide linker (HQNKKGGSGDGKKKQHQ). Each resultant ZFP gene was cloned into the plasmid pMal (New England Biolabs, Beverly, Massachusetts) as a fusion with DNA encoding maltose-binding protein. Protein was isolated and binding studies done as described² with slightly modified buffer conditions (under these conditions SP1 shows a higher affinity than that seen in previous studies). ZFP concentrations were determined directly by measuring the DNA-binding activity of each ZFP preparation using conditions under which binding is essentially stoichiometric (concentrations of ZFP and target site >50 \times K_d).

Construction of ZFP-based transcription factors and vectors. To construct expression plasmids encoding *Vegfa*-activating ZFPs, the cassettes encoding each three- or six-finger ZFP were assembled by PCR with genes encoding the nuclear translocation signal from SV40 large T antigen, the herpes simplex virus VP16 transactivation domain spanning amino acids 413–490 and a FLAG peptide. They were subcloned into pcDNA3.1 (Clontech, Palo Alto, California) with expression under direction of the CMV promoter. Recombinant adenovirus vectors were constructed using the Ad-Easy system²¹. The MMLV-based retroviral vectors were derived from pLXSN, which contains a neomycin-resistance gene under the control of an internal SV40 promoter. The LXSN vectors were produced in the 293 Amphi-Pak cell line (Clontech).

In vitro studies. To produce stable ZFP expressing cells, 293 Amphi-Pak and C127I cells (ATCC) were transduced with ZFP-encoding retrovirus and G418-resistant populations of cells were established 14 d later. Cells were plated (5 \times 10³ cells per well) and *Vegfa* expression evaluated by ELISA (R&D Systems, Palo Alto, California) on medium collected from wells 24 h after re-feeding. Adenovirus constructs were tested *in vitro* by transduction of rat aortic smooth muscle cells. At 24 h after transduction, cells were scraped and lysates used for western-blot analysis of VP16 and FLAG expression (see below).

In vivo skeletal muscle transduction. Adenovirus encoding *Vegfa*-ZFP was injected intramuscularly into the quadriceps of CD-1 mice (10⁸ PFU in 50 μ l PBS) using a 27-gauge needle. Control vector was injected into the contralateral quadriceps. Plasmid DNA injection was done similarly using 50 μ g of DNA. Mice were sacrificed after 3 d and muscle harvested for analysis of gene expression. Western blotting was done starting with muscle lysates using a monoclonal antibody against VEGF-A (Research Diagnostics, Flanders, New Jersey) and an ECL kit. Antibodies against FLAG (Sigma, St. Louis, Missouri) and the VP16 transactivation domain (Santa Cruz Biotechnology, Santa Cruz, California) were used to determine expression of the ZFPs. Antibody against actin was used to control for loading. For real-time quantitative RT-PCR (QRT-PCR), RNA was isolated using Trizol (Invitrogen, Carlsbad, California), treated with DNase I and purified again using RNeasy (Qiagen, Valencia, California). QRT-PCR was done essentially as previously described²². All samples (n = 4 HIF-1 α , 4 ZFP, 8 contralateral controls) were amplified in duplicate and values averaged for analysis. QRT-PCR of 18S RNA was used for standardization.

Ear angiogenesis and wound healing studies. Ear angiogenesis studies were a modification of an approach described previously¹². Adenovirus vectors encoding either a *Vegfa*-activating ZFP or murine *Vegfa*₁₆₄ were injected subcutaneously into the ears of CD-1 mice (10⁸ PFU in 1.5 μ l). Contralateral ears were injected with adeno-GFP. Digital photographs were obtained after 3 or 6 d. Evans blue dye (200 μ l of 4% solution) was injected in the tail vein and the distribution in the ears was assessed and photographed 3 h later. Frozen sections (5 μ m) were immunostained with a monoclonal anti-

body against the endothelial-cell marker PECAM and vessel counts obtained as described²². QRT-PCR analysis was carried out with RNA isolated from ears 3 d after transduction using splice variant-specific and splice variant-nonspecific primer-probe pairs to differentiate between the amounts of total and splice-variant Vegfa mRNA.

Cutaneous wounds were created by using a 5-mm round punch biopsome essentially as described¹⁴. Duplicate wounds were created on contralateral flanks of CD-1 mice and treated with adenovirus encoding either mVZ-57 or GFP (10⁸ PFU in 25 μ l PBS). After 5 d, wounds were excised, bisected exactly in the center and embedded in paraffin. Serial 5- μ m sections were stained with H&E. Re-epithelialization was assessed by measuring the distance between the leading edges of keratinocyte ingrowth on digital images. Alternate sections were immunostained and vessel counts obtained as described²². Studies were carried out under approved animal protocols approved by the Yale University animal care and use committee.

Acknowledgements

The authors thank A. Wolffe whose essential scientific input and discussions made this work possible; C. Pabo for scientific input and helpful comments on the manuscript; E. Lanphier and D. Bobo for supporting the ZFP concept; and A. Vincent for technical assistance. This work was funded by an American Heart Association award (AHA no. 97-30083N), by US National Institutes of Health grant RO1-HL64001 and by an unrestricted gift from Edwards Lifesciences (all to F.J.G.).

Competing financial interests

The authors declare competing financial interests: see the website (<http://www.nature.com/naturemedicine>) for details.

RECEIVED 26 AUGUST; ACCEPTED 1 OCTOBER 2002

1. Pabo, C. O., Peisach, E. & Grant, R. A. Design and selection of novel Cys₂His₂ zinc finger proteins. *Annu. Rev. Biochem.* **70**, 313–340 (2001).
2. Liu, P. Q. *et al.* Regulation of an endogenous locus using a panel of designed zinc finger proteins targeted to accessible chromatin regions. Activation of vascular endothelial growth factor A. *J. Biol. Chem.* **276**, 11323–11334 (2001).
3. Zhang, L. *et al.* Synthetic zinc finger transcription factor action at an endogenous chromosomal site. Activation of the human erythropoietin gene. *J. Biol. Chem.* **275**, 33850–33860 (2000).
4. Beerli, R. R., Segal, D. J., Dreier, B. & Barbas, C. F. III. Toward controlling gene ex-

pression at will: Specific regulation of the erbB-2/HER-2 promoter by using poly-dactyl zinc finger proteins constructed from modular building blocks. *Proc. Natl. Acad. Sci. USA* **95**, 14628–14633 (1998).

5. Jamieson, A. C., Kim, S. H. & Wells, J. A. In vitro selection of zinc fingers with altered DNA-binding specificity. *Biochemistry* **33**, 5689–5695 (1994).
6. Pavletich, N. P. & Pabo, C. O. Zinc finger-DNA recognition: Crystal structure of a Zif268-DNA complex at 2.1 \AA . *Science* **252**, 809–817 (1991).
7. Choo, Y. & Klug, A. Selection of DNA binding sites for zinc fingers using rationally randomized DNA reveals coded interactions. *Proc. Natl. Acad. Sci. USA* **91**, 11168–11172 (1994).
8. Greisman, H. A. & Pabo, C. O. A general strategy for selecting high-affinity zinc finger proteins for diverse DNA target sites. *Science* **275**, 657–661 (1997).
9. Desjarlais, J. R. & Berg, J. M. Use of a zinc-finger consensus sequence framework and specificity rules to design specific DNA binding proteins. *Proc. Natl. Acad. Sci. USA* **90**, 2256–2260 (1993).
10. Rebar, E. J. & Pabo, C. O. Zinc finger phage: Affinity selection of fingers with new DNA-binding specificities. *Science* **263**, 671–673 (1994).
11. Wolffe, A. P. *Chromatin Structure and Function* (Academic Press, London, 1998).
12. Pettersson, A. *et al.* Heterogeneity of the angiogenic response induced in different normal adult tissues by vascular permeability factor/vascular endothelial growth factor. *Lab. Invest.* **80**, 99115 (2000).
13. Thurston, G. *et al.* Angiopoietin-1 protects the adult vasculature against plasma leakage. *Nature Med.* **6**, 460–463 (2000).
14. Low, Q. E. H. *et al.* Wound healing in MIP-1 α and MCP-1 α mice. *Am. J. Pathol.* **159**, 457–463 (2001).
15. Grunstein, J., Masbad, J. J., Hickey, R., Giordano, F. J. & Johnson, R. S. Isoforms of vascular endothelial growth factor act in a coordinate fashion to recruit and expand tumor vasculature. *Mol. Cell. Biol.* **20**, 7282–7291 (2000).
16. Elson, D. A. *et al.* Induction of hypervascularity without leakage or inflammation in transgenic mice overexpressing hypoxia-inducible factor-1. *Genes Dev.* **15**, 2520–2532 (2001).
17. Giordano, F. J. *et al.* Intracoronary gene transfer of fibroblast growth factor-5 increases blood flow and contractile function in an ischemic region of the heart. *Nature Med.* **2**, 534–539 (1996).
18. Vale, P. R. *et al.* Left ventricular electromechanical mapping to assess efficacy of hVEGF₁₆₅ gene transfer for therapeutic angiogenesis in chronic myocardial ischemia. *Circulation* **102**, 965–974 (2000).
19. Rosengart, T. K. *et al.* Angiogenesis gene therapy: Phase I assessment of direct intramyocardial administration of an adenovirus vector expressing VEGF₁₂₁ cDNA to individuals with clinically significant severe coronary artery disease. *Circulation* **100**, 468–474 (1999).
20. Vincent, K. A. *et al.* Angiogenesis is induced in a rabbit model of hindlimb ischemia by naked DNA encoding an HIF-1 α /VP16 hybrid transcription factor. *Circulation* **102**, 2255–2262 (2000).
21. He, T. C. *et al.* A simplified system for generating recombinant adenoviruses. *Proc. Natl. Acad. Sci. USA* **95**, 2509–2514 (1998).
22. Giordano, F. J. *et al.* A cardiac myocyte vascular endothelial growth factor paracrine pathway is required to maintain cardiac function. *Proc. Natl. Acad. Sci. USA* **98**, 5780–5785 (2001).